water

MDPI

Article

A Half-Century of Human Impact on Nan River Runoff and Sediment Load Supplied to the Chao Phraya River

Matharit Namsai [1,2], Butsawan Bidorn [1,3,*], Ruetaitip Mama [2] and Warit Charoenlerkthawin [1,3]

[1] Department of Water Resources Engineering, Chulalongkorn University, Bangkok 10330, Thailand; matharit.na@student.chula.ac.th (M.N.); w.charoenlerkthawin@gmail.com (W.C.)
[2] Royal Irrigation Department, Bangkok 10300, Thailand; ruetaitip.mama@gmail.com
[3] Center of Excellence in Interdisciplinary Research for Sustainable Development, Chulalongkorn University, Bangkok 10330, Thailand
* Correspondence: butsawan.p@chula.ac.th; Tel.: +66-2218-6455

Abstract: The construction of large dams in the upper tributary basin of the Chao Phraya River (CPR) has been linked to a significant decrease in sediment load in the CPR system, estimated between 75–85%. This study, utilizing historical and recent river flow and sediment data from 1922 to 2019, examines the impact of three major dams constructed in the Nan River basin (the Sirikit, Naresuan, and Khwae Noi dams) on river runoff and sediment loads in the CPR. The investigation employed the Mann–Kendall (MK) test and the double mass curve (DMC) for analysis. Findings indicate that the Nan River is a major contributor to the CPR, accounting for around 40% of the runoff and 57% of the total sediment load (TSL). The Naresuan diversion dam's water regulation was found to significantly reduce annual runoff and TSL downstream of the dam. Despite an initial increase in sediment load at the CPR headwater (C.2) post the construction of the Sirikit dam, attributed to expanded irrigation downstream and channel improvements in the lower Nan River, the operation of the three dams eventually led to a 31% reduction in sediment load at C.2 compared to pre-construction levels.

Keywords: runoff; environmental impact of dams; river surveying; hydrological regime; environmental change

Citation: Namsai, M.; Bidorn, B.; Mama, R.; Charoenlerkthawin, W. A Half-Century of Human Impact on Nan River Runoff and Sediment Load Supplied to the Chao Phraya River. *Water* **2024**, *16*, 148. https://doi.org/10.3390/w16010148

Academic Editor: Paolo Mignosa

Received: 11 December 2023
Revised: 25 December 2023
Accepted: 28 December 2023
Published: 30 December 2023

1. Introduction

Rivers serve as crucial conduits connecting continents to oceans, transferring substantial quantities of terrestrial materials such as freshwater, sediments, nutrients, and notably, carbon into the global ocean [1–4]. Alterations in streamflow and sediment load have a profound impact on fluvial dynamics, delta development, and riverine as well as coastal biogeochemical cycles [5,6]. It has been posited in prior research that shifts in river discharge and sediment load, primarily driven by climatic variations and human activities, can lead to significant socio-economic impacts [7,8]. Over recent decades, human-induced changes, including deforestation, dam construction, water diversion, and sand mining, have been implicated in the alteration of river runoffs and sediment fluxes [9–13], consequently influencing sediment deposition in the oceans [5,6,14].

Dams, a prevalent feature in global water management systems, can lead to sediment accumulation within their reservoirs, thereby modifying downstream river flow and sediment transport [15–21]. Major rivers worldwide have experienced sediment reductions ranging from 40–98% due to damming, with negligible changes in annual river runoff. Examples include the Yangtze River [17,19,22], the Nile River [10,23], the Red River [15,21], and the Mekong River [18]. The impact of dam construction on sediment load varies from river to river, influenced by factors such as geological setting, hydrological conditions, dam location, and water management practices [24–26]. Given that riverine sediments are key in shaping coastal morphology and shoreline evolution, understanding the changes in

runoff and sediment load due to damming is essential for sustainable river and coastal management [14,27,28].

The Chao Phraya River (CPR) (Figure 1), central to the largest river basin in Thailand and the fifth largest in Southeast Asia [14], has been a key fluvial conduit to the Gulf of Thailand, shaping the Chao Phraya Delta (CPD) with a sedimentation rate of 1.5 km^2/y for the last two millennia [29]. Over the past sixty years, however, the CPD has undergone significant coastal erosion, with an average shoreline retreat rate of over −7 m/y [14,30–32]. The Greater Chao Phraya Project commenced in 1952, marking Asia's most ambitious water development initiative at the time. This project included the construction of the Bhumibol Dam on the Ping River (completed in 1964), the Sirikit Dam on the Nan River (completed in 1972), and numerous other water management infrastructures across the Greater Chao Phraya River basin [28]. An analysis of historical sediment data from hydrological station C.2 (Figure 1a) indicates that the building of the Bhumibol and Sirikit Dams significantly reduced the annual sediment supply to the CPR by 75–85%, contributing to the CPD's shoreline recession [31–36]. Namsai et al. [12] noted that the Bhumibol Dam's construction led to a 5% decrease in annual sediment yield and minimal impact on river discharge from the Ping tributary (P.17) to the CPR. Similarly, the construction of the Kiew Lom, Mae Chang, and Kiew Koh Ma dams in the Wang River basin did not markedly alter the streamflow and sediment load from the Wang River (W.4A) to the CPR [25]. Furthermore, sediment loads in the Yom River (Y.16) remained stable despite the construction of a major barrage (the Mae Yom Barrage) on the river's main course [37].

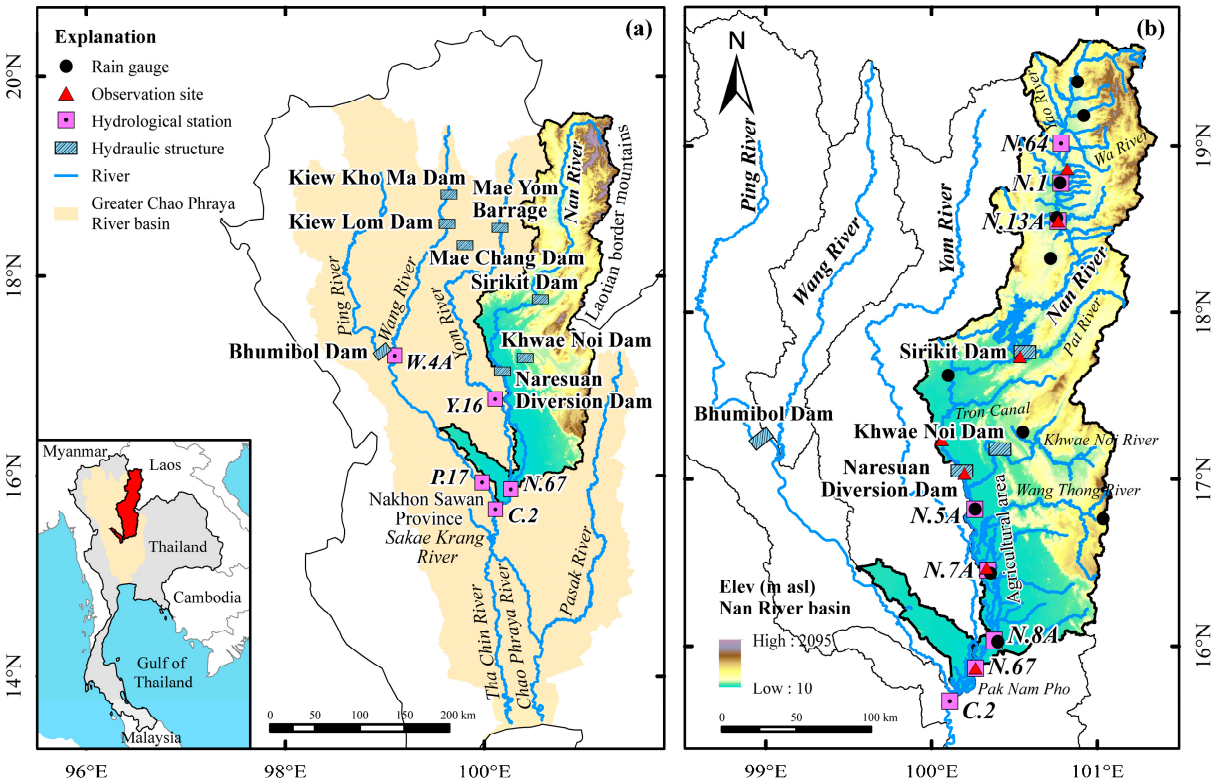

Figure 1. Geographical illustration of Thailand's extensive Chao Phraya River Basin: (**a**) the Nan River watershed highlighting the positions of major dams within the Chao Phraya River network; (**b**) sites of hydrological monitoring managed by the Royal Irrigation Department (RID) and the observation sites in this study.

The Nan River basin is one of the four major basins (the Ping, Wang, Yom, and Nan River basins) forming the CPR. The basin experiences a dry season from November to mid-March due to the northeast monsoon and a wet season from mid-May to mid-October influenced by the southwest monsoon. It has an average annual rainfall of 1287 mm, with 90% during the wet season [38]. The basin contributes 38% to the CPR's annual runoff, totaling about 12,000 $\times$ 10^6 m^3/y [38]. Over 920 water management projects in the basin support irrigation, hydroelectric power, flood control, fisheries, and the prevention of saltwater intrusion. Major projects include the Sirikit Dam, the Naresuan diversion dam, and the Khwae Noi Dam. The Sirikit Dam, the second-largest in the CPR and third-largest in Thailand with a capacity of 9510 $\times$ 10^6 m^3, is located 460 km from the basin's outlet and was completed in 1972 for multiple purposes [39]. The Naresuan Dam, a diversion dam finished in 1985 about 275 km from the basin's outlet, aids in irrigation and water management [38]. Lastly, the Khwae Noi Dam, established in 2011 with a capacity of 939 $\times$ 10^6 m^3, is situated about 240 km from the basin's outlet and aimed at flood mitigation and agricultural water supply [40].

Previous research has found no significant long-term trends in annual runoff and sediment load from the Ping and Wang rivers to the CPR [12,25], whereas an increasing trend in both runoff and sediment load was observed in the Yom River [37]. In contrast, a notable decreasing trend in sediment load was detected at station C.2 in the CPR [12,25]. Given the Nan River's status as the CPR's largest tributary, this reduction at C.2 might be attributed to changes in the Nan River's sediment flux, potentially linked to the construction of major dams like the Sirikit Dam, the Naresuan diversion dam, and the Khwae Noi Dam. Yet, detailed studies on sediment characteristics and variations in the Nan River are lacking. Recognizing rivers as intricate, nonlinear, dynamic systems [41] and acknowledging the pivotal importance of river sediment data in water management and environmental assessment, this study was undertaken with three key objectives: Firstly, it seeks to explore the sediment characteristics along the Nan River. Secondly, this study analyzes the temporal and spatial variations in streamflow and sediment load within the Nan River. Lastly, it aims to assess the impacts of three major dams—the Sirikit, Naresuan, and Khwae Noi dams—on the runoff and sediment load of the Nan River as it finally drains into the CPD. This research seeks to deepen our understanding of how damming and human activities influence sediment transport in the Nan River and the broader CPR system.

2. Materials and Methods

2.1. Study Area

Spanning approximately 34,680 km^2, the Nan River basin is the largest of the four major basins (including the Ping, Wang, Yom, and Nan River basins) that constitute the Chao Phraya River (CPR) system. It lies in northern Thailand, between latitudes 15°42′ and 18°37′ N, and longitudes 99°51′ to 101°21′ E [38], as depicted in Figure 1a. The Nan River, originating from the Luang Phra Bang Mountain at the eastern edge of the Thai highlands, flows south through the upper northern valleys and the lower north's flatlands, eventually converging with the Ping River to form the CPR in Nakhon Sawan Province [42–44] (Figure 1b). The river's gradient, varying from 1:500 to 1:14,300, is illustrated in Figure 2, with the main river stretching about 770 km [44–47]. The basin's terrain is categorized into three sections [38,45]: the upper basin, upstream of hydrological station N.13A, is mountainous with a river channel 100–200 m wide and 7–12 m deep, and a gradient between 1:500 and 1:3000. The middle basin, located between stations N.13A and N.5A, features highlands with a river gradient from 1:1430 to 1:5000 and a width of 150–220 m, at depths of 8–10 m. Lastly, the lower basin, downstream of station N.5A, includes floodplain areas with gentler slopes of about 1:14,300 and river dimensions ranging from 100–150 m wide and 10–17 m deep.

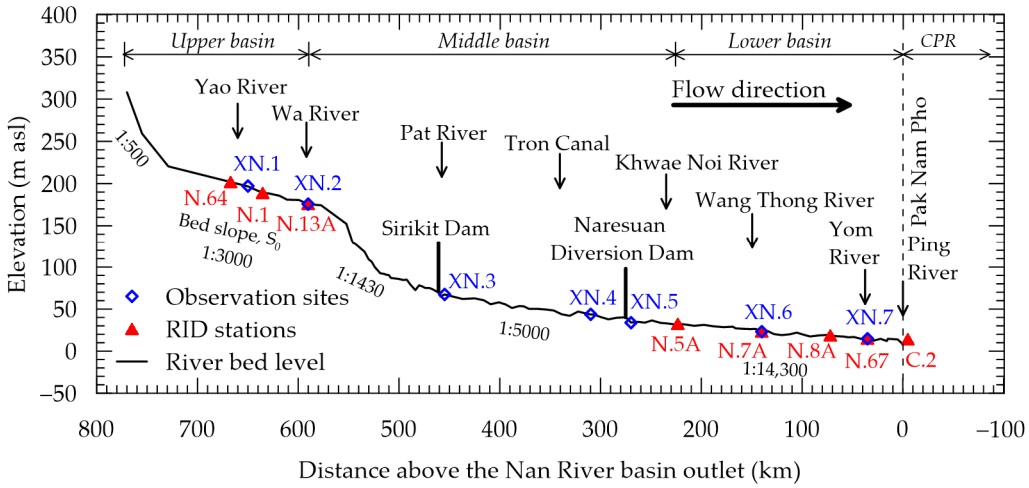

Figure 2. Profile view of the Nan River detailing the positions of RID hydrological monitoring stations (indicated by red triangles) and sites of field observations (marked with blue diamonds). The zero mark on the x-axis represents the confluence of the Ping and Nan rivers.

2.2. Assessing of Fluvial Discharge and Sedimentary Load

In the study of the Nan River basin's sediment dynamics, comprehensive hydrographic surveys were carried out at seven strategic locations along the river, designated XN.1 through XN.7 in Figure 2, to gather essential data on river discharge and sediment load. The surveys, executed during the contrasting periods of the wet and dry seasons of 2018, targeted the upper (XN.1 and XN.2), middle (XN.3–XN.5), and lower (XN.6 and XN.7) reaches of the river. These assessments recorded a range of variables including water flow, area, velocity, depth, and suspended sediment concentration, as well as bedload and bed material.

River discharge and flow area were precisely quantified using an Acoustic Doppler Current Profiler (ADCP), specifically the Sontek River Surveyor M9 model (Sontek, San Diego, CA, USA), which boasts an accuracy of ± 0.25 cm/s for velocity and 1% for depth. Suspended sediment load (SSL) was evaluated using a depth-integrating sampler, with the US D-49 model (Performance Results Plus Inc., Columbus, OH, USA) employed for deeper sections and the US DH-48 (Performance Results Plus Inc., Columbus, OH, USA) for shallower ones where manual crossing was possible. The river's breadth was divided into segments of equal width, ranging from five to eleven, to ensure comprehensive sample collection. Water samples were gathered in a vertical direction from the bed to the surface to capture a representative sediment concentration, which was then analyzed in a soil laboratory as per procedures outlined in Edwards et al. [48].

For bedload (BL) measurement, the well-established Helley-Smith (U.S. BL-84) sampler (Performance Results Plus Inc., Columbus, OH, USA) was utilized [49], adhering to a specified sampling duration. The sediment samples were processed in a laboratory, dried, and segregated via sieving to determine the granulometry as per standard soil particle-size analysis protocols detailed in Namsai et al. [12]. Additionally, the riverbed material was collected from three equidistant points across the river section using a Van Veen grab to acquire surface samples up to 20 cm deep, which were then analyzed for grain size distribution following the same method as the bedload samples. The compiled data on SSL and BL at each section were computed by integrating the sediment concentration with the flow metrics, adhering to methodologies reported in previous studies [12,50,51].

2.3. Identifying Changes and Patterns in Fluvial Discharge and Sediment Transports

To analyze fluctuations in river discharge and sediment load in the Nan River, a historical dataset of daily river discharge and suspended sediment load from 1922 to 2019 was sourced from the Royal Irrigation Department (RID). The dataset encompassed

daily flow and sediment information gathered at eight hydrological stations (N.64, N.1, N.13A, N.5A, N.7A, N.8A, N.67, and C.2, as depicted in Figure 1b). The stations N.64, N.1, and N.13A monitor the upper basin, station N.5A surveys the middle basin, and stations N.7A, N.8A, and N.67 are responsible for the lower basin. For this research, observations from Station C.2, positioned 5 km downstream from the CPR confluence, were pivotal in evaluating dam impacts on sediment delivery from the Nan River into the CPR. A compilation of the discharge and SSL data specifics for each station is provided in Table 1. In the absence of direct BL data, the TSL for the Nan River system was inferred using sediment rating curves combined with bed-to-suspended sediment ratios, based on the river survey data mentioned in Namsai et al. [12].

Table 1. River flow and sediment data at hydrological stations along the Nan and Chao Phraya rivers provided by the RID.

Station	[1] Dist.	Drainage	Data	Period	Max.	Ave.	Min.	[4] S.D.
(River)	(km)	(km^2)						
N.64	+667	3432	[2] Q_w (m^3/s)	1994–2019	2281	82	2	135
(Nan)			[3] Q_s (t/d)	2007–2019	199,765	3053	~0	10,038
N.1	+635	4609	Q_w (m^3/s)	1922–2019	2636	100	1	171
(Nan)			Q_s (t/d)	1978–2019	324,347	2966	~0	12,853
N.13A	+590	8784	Q_w (m^3/s)	1959–2019	4764	197	3	335
(Nan)			Q_s (t/d)	1994–2007	230,624	5593	19	14,138
N.5A	+223	25,286	Q_w (m^3/s)	1951–2019	2159	244	3	263
(Nan)			Q_s (t/d)	1978–2019	141,502	2641	10	6018
N.7A	+140	29,153	Q_w (m^3/s)	1944–2019	1786	320	5	320
(Nan)			Q_s (t/d)	2001–2019	56,373	3566	155	5356
N.8A	+72	31,472	Q_w (m^3/s)	1952–2019	2116	327	1	323
(Nan)			Q_s (t/d)	1997–2019	54,619	3711	135	5015
N.67	+35	57,384	Q_w (m^3/s)	1998–2019	1579	418	33	340
(Nan)			Q_s (t/d)	1999–2019	30,267	5620	84	5904
C.2	–5	109,973	Q_w (m^3/s)	1956–2019	5450	711	15	695
(CPY)			Q_s (t/d)	1965–2019	493,805	13,705	236	27,596

Note: [1] Distance from the Nan River outlet is denoted by a positive (+) sign indicating the upstream direction from the outlet, and a negative (–) sign indicating the downstream direction; [2] Q_w represents the river discharge measured in cubic meters per second (m^3/s); [3] Q_s denotes the suspended sediment load recorded in tons per day (t/d); [4] S.D. refers to the standard deviation.

To discern trends in the annual streamflow and sediment series, the Mann–Kendall (MK) test, a non-parametric statistical approach, was employed [52,53]. This test is particularly suited to hydro-meteorological series that exhibit skewness or are incomplete [11,54–56]. The MK test assesses the sequence of $X(x_1, x_2, \ldots, x_n)$ through the MK statistic, S, as expressed in Equation (1). The analysis used annual totals compiled from daily measurements spanning from the 1st of April to the 31st of March of each following year, aligning with Thailand's hydrological year.

$$S = \sum_{i=1}^{n-1} \sum_{j=i+1}^{n} sgn(X_j - X_i) \quad (1)$$

where the X_j is the sequential data values, n is the length of the dataset, and $sgn(\theta)$ can be calculated using Equation (2).

$$sgn(\theta) = \begin{cases} 1, \ if \ \theta > 0 \\ 0, \ if \ \theta = 0 \\ -1, \ if \ \theta < 0 \end{cases} \quad (2)$$

For datasets where n is 8 or greater, the S statistic is presumed to follow a normal distribution. The expected mean and variance for this distribution are provided in Equations (3) and (4), respectively.

$$E[S] = 0 \tag{3}$$

$$V(S) = \frac{n(n-1)(2n+5) - \sum_{i=1}^{m} t_i i(i-1)(2i+5)}{18} \tag{4}$$

where m is the number of groups of tied ranks, and t_i denotes the count of tied groups of size i.

The computation of the normalized test statistic (Z) for the MK test, along with the associated one-tailed p-value (p), is outlined in Equations (5) through (7).

$$Z = \begin{cases} \frac{S-1}{\sqrt{V(S)}}, & if\ S > 0 \\ 0, \quad if\ S = 0 \\ \frac{S+1}{\sqrt{V(S)}}, & if\ S < 0 \end{cases} \tag{5}$$

$$p = 0.5 - \Phi(|Z|) \tag{6}$$

$$(\Phi|Z|) = \frac{1}{\sqrt{2\pi}} \int_0^{|Z|} e^{\frac{-t^2}{2}} dt \tag{7}$$

A positive Z value signifies a rising trend, whereas a negative Z value suggests a decreasing trend. A p-value at or below 0.05 denotes a trend that is statistically significant at the 5% significance level [54].

2.4. Evaluating the Impact of Human Activities on Fluvial Discharge and Sediment Load

To evaluate human influence on river flow and sediment transport, the double mass curve (DMC) method is commonly applied [17,57]. A DMC plots the accumulated totals of two interrelated variables over time, revealing their proportional relationship [58]. A linear relationship on the graph indicates consistent proportionality, while any deviation or curve inflection points to a shift in this relationship or a change in the slope of the DMC [59].

In this analysis, to evaluate the influence of the three significant dams on annual river flow, DMCs of cumulative annual precipitation against cumulative annual river flow were charted for periods before and after the dams were constructed along the Nan River. For assessing the impact on sediment load, DMCs comparing cumulative annual river discharge with cumulative annual TSL were created, encompassing eras preceding and succeeding the dam constructions. Annual rainfall data was summed from daily records within the Thai water year, with a quality check in place to exclude any data that significantly deviated from long-term trends and to interpolate missing entries using adjacent station data or relevant time series. The Thiessen polygon technique was utilized to determine the average rainfall over the catchment area pertinent to each hydrologic station [60].

3. Results

3.1. Hydrology and Sedimentology of the Nan River from 2018 Field Data

Data on river hydrology and sediment characteristics gathered at sites XN.1 to XN.7 of the Nan River during the 2018 dry and wet seasons are reported in Table 2. Concurrently, Figure 3 graphically represents the variations in river discharge, SSL, BL, and bed material grain size at these monitoring sites. The findings from the upper (XN.1 and XN.2), middle (XN.3–XN.5), and lower stretches (XN.6 and XN.7) of the river are summarized in Table 2.

Table 2. River flow and sediment data observed along the Nan River in 2018.

Site	Dist. (km)	[1] A (m^2)	[2] V (m/s)	[3] Q_w (m^3/s)	[4] Q_s (t/d)	[5] Q_b (t/d)	[6] Q_t (t/d)	Q_b/Q_s (%)	Q_b/Q_t (%)	d_{50} (mm)
Dry season										
XN.1	650	55	0.15	8.1	6.2	0	6.2	0	0	1.79
XN.2	590	96	0.19	18.1	7.7	0	7.7	0	0	3.89
XN.3	455	143	0.05	6.7	10.8	0	10.8	0	0	1.12
XN.4	310	577	0.45	259.2	501.7	18.4	520.1	3.7	3.5	0.66
XN.5	270	263	0.52	137.7	228.5	24.5	253.0	10.7	9.7	2.07
XN.6	140	302	0.78	236.8	814.2	310.6	1124.8	38.2	27.6	0.80
XN.7	35	478	0.51	241.6	1168.9	12.7	1181.6	1.1	1.1	0.94
Wet season										
XN.1	650	654	1.34	873.4	75,391.8	6.8	75,398.6	~0	~0	1.49
XN.2	590	1512	0.95	1439.8	82,393.2	172.9	82,566.1	0.2	0.2	0.90
XN.3	455	194	0.23	44.6	608.5	0	608.5	0	0	1.05
XN.4	310	523	0.52	272.4	2452.6	45.8	2498.4	1.9	1.8	0.25
XN.5	270	133	1.69	224.7	1681.6	1.5	1683.1	0.1	0.1	0.15
XN.6	140	435	0.80	349.2	3269.6	67.2	3336.8	2.1	2.0	0.56
XN.7	35	656	0.81	532.0	8380.3	22.0	8402.3	0.3	0.3	0.38

Note: [1] A denotes the cross-sectional area of flow; [2] V represents the velocity of water flow; [3] Q_w stands for river discharge; [4] Q_s indicates the amount of suspended sediment load; [5] Q_b refers to the bedload; [6] Q_t is the aggregate sediment load. The term d_{50} is used to describe the median diameter of sediment grains.

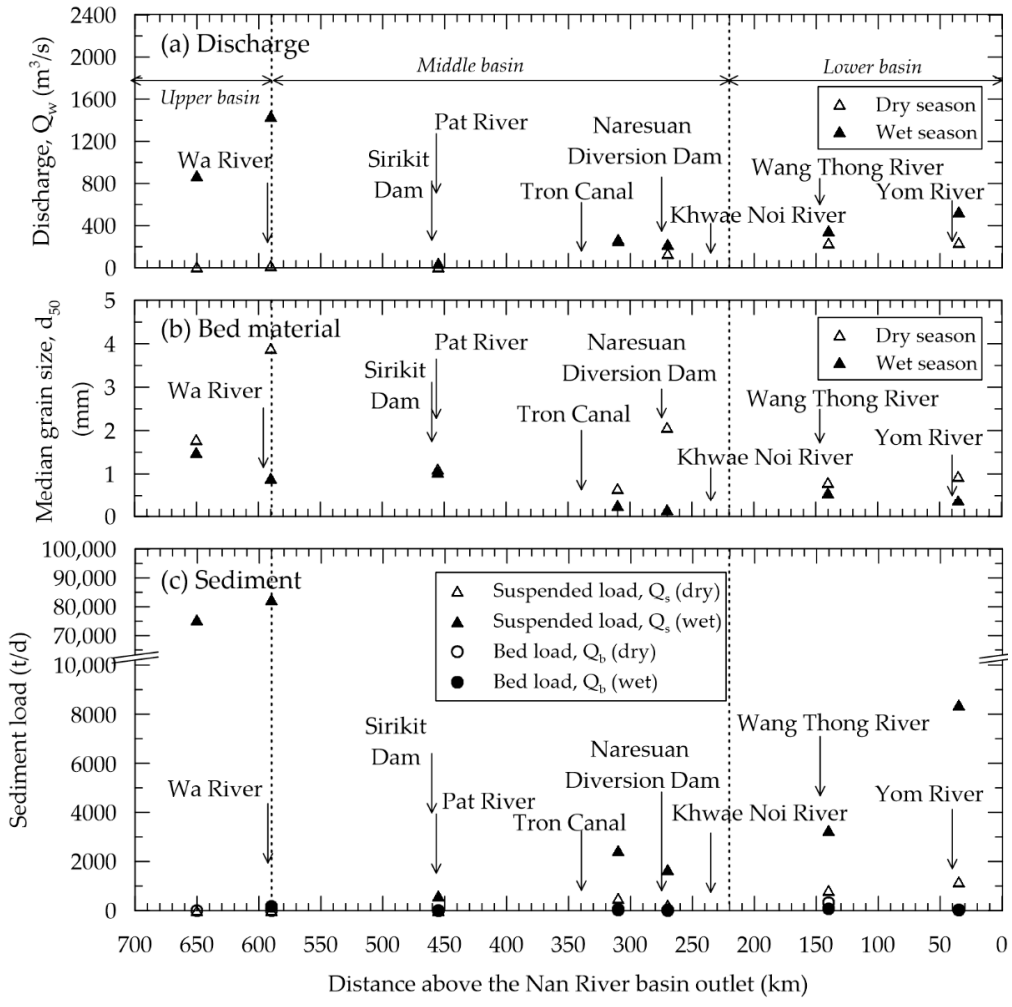

Figure 3. Hydrological and sediment data measured along the Nan River in 2018: (**a**) flow rates; (**b**) median bed material size (d_{50}); (**c**) suspended sediment and bed loads.

During the 2018 dry season, the upper Nan River's flow, positioned upstream of the Sirikit Dam, exhibited an increase from 8.1 to 18.1 m^3/s. Progressing through the middle reach, flows augmented from 6.7 to 259.2 m^3/s but dipped to 137.7 m^3/s past the Naresuan diversion dam. The lower basin's flow slightly rose from 236.8 to 241.6 m^3/s, as depicted in Figure 3a. As detailed in Figure 3b, sediment at the upper reach was predominantly very coarse sand to very fine gravel, with median grain sizes ranging between 1.79 and 3.89 mm. The middle and lower reaches were primarily composed of coarse to very coarse sand, with median grain sizes of 0.66 to 2.07 mm. In terms of SSL, upper basin measured data showed an increase from 6.2 to 7.7 t/d. The middle basin's SSL figures followed the river's flow pattern, climbing from 11 to 502 t/d, then reducing to 229 t/d beyond the Naresuan Dam. In the lower basin, SSL elevated from 814 to 1169 t/d. According to Table 2, the upper reach's BL was below the detectable level during this period. In contrast, BL observed data in the middle reach showed an upsurge from non-detectable levels to 25 t/d, while the lower reach experienced a reduction from 311 to 13 t/d, as illustrated in Figure 3c. Furthermore, the BL-to-SSL ratios exhibited variability, ranging between non-detectable to 0.11 in the middle reach and 0.01 to 0.38 in the lower reach, as indicated in Table 2.

During the wet season, flow rates in the Nan River's upper basin showed an uptrend, varying from 873.4 to 1439.8 m^3/s, then sharply decreased at station XN.3 in the middle reach to 45 m^3/s, a change attributed to the Sirikit Dam's operations. Flows then increased to 272.4 m^3/s before the Naresuan diversion dam and subsequently declined to 224.7 m^3/s past it, likely due to upstream water diversions. Further downstream, the flow again rose, reaching 532 m^3/s. Wet season bed materials were finer than in the dry season, with median grain sizes ranging from 0.9 to 1.49 mm in the upper reaches and 0.15 to 1.05 mm in the middle reaches, shifting to 0.38 to 0.56 mm in the lower basin. The SSL patterns mirrored the dry season, increasing downstream, while BL showed variability, with an increase in the upper reaches and a fluctuating pattern in the middle and lower reaches. The BL-to-SSL ratios also varied across the basin, with the lowest in the upper reaches and slightly higher values downstream (as summarized in Table 2 and illustrated in Figure 3).

3.2. Historical Fluvial Discharge and SSL Data of the Nan River

An analysis of the long-term daily river flow and SSL data, recorded at various RID hydrological stations from 1922 to 2019, is presented in Table 1. Time series representations of the annual river discharge and SSL are provided in Figures 4 and 5, respectively.

Figure 4 illustrates a downstream increase in river discharge, beginning at 82 m^3/s (N.64) and ascending to 418 m^3/s (N.67; situated 35 km from the river basin's outlet). The examination of daily river flow (referenced in Table 1) reveals a downstream augmentation in the upper basin, with discharge rates ranging from 82 (N.64) to 197 m^3/s (N.13A). In the middle basin at N.5A, the discharge reached 244 m^3/s, and in the lower reach (N.7A, N.8A, and N.67), the flow rate exhibited an increase from 320 to 418 m^3/s. Observations at C.2, positioned 5 km downstream of the confluence where the Ping and Nan rivers merge to form the CPR (as seen in Figure 1), showed a marked increase in discharge to 711 m^3/s (as detailed in Table 1).

The historical sediment data outlined in Table 1 reveal a marginal increase in SSL moving downstream. In the upper basin, the SSL averages grew from 3053 t/d at N.64 to 5593 t/d at N.13A, followed by a slight decrease to 2641 t/d in the middle basin at N.5A. Progressing downstream, the lower basin's SSL averages rose from 3566 to 5620 t/d. At C.2, the SSL was significantly higher, averaging 13,700 t/d, which is approximately 2.4 times the mean SSL emanating from the Nan River.

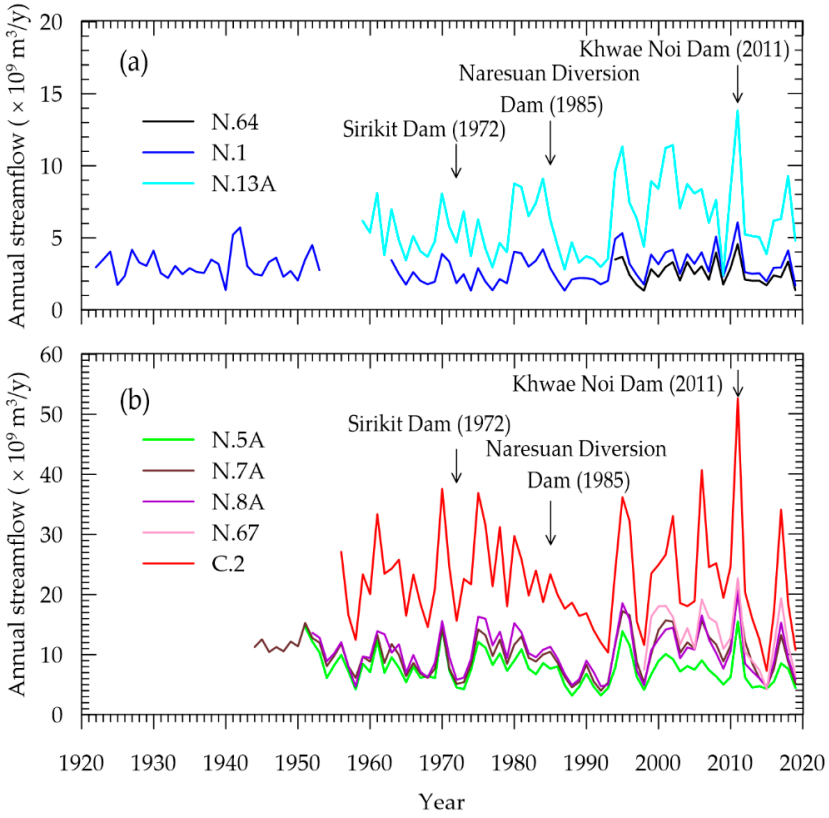

Figure 4. Annual streamflow observed at the RID hydrological stations during 1922–2019: (**a**) N.64, N.1, and N.13A; (**b**) N.5A, N.7A, N.8A, N.67, and C.2.

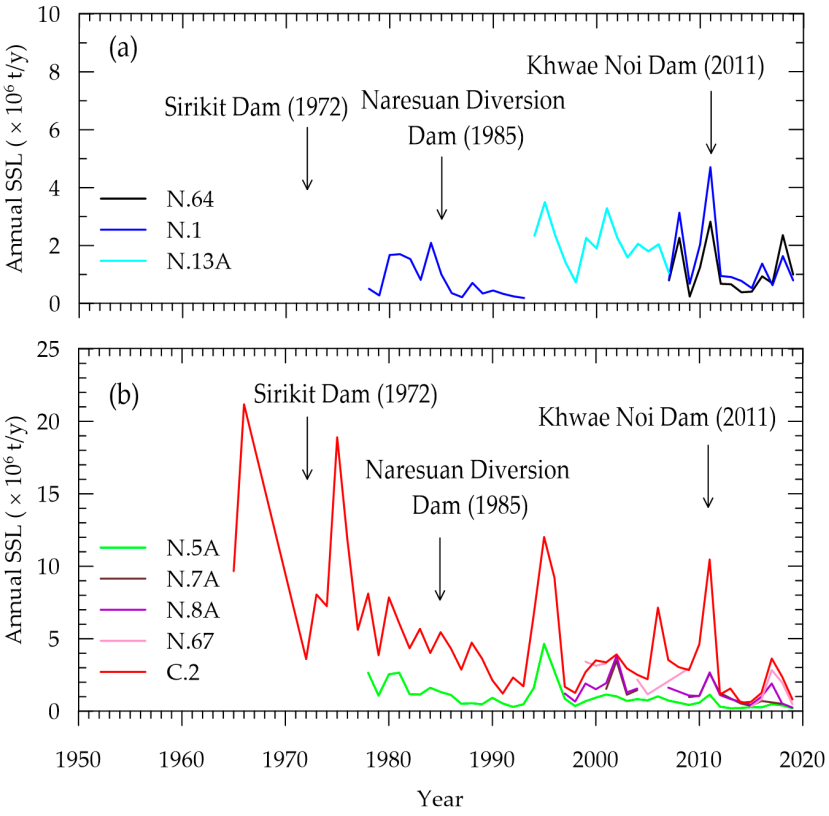

Figure 5. Annual suspended sediment data observed at the RID hydrological stations during 1965–2019: (**a**) N.64, N.1, and N.13A; (**b**) N.5A, N.7A, N.8A, N.67, and C.2.

Correlation plots derived from historical daily river discharge against SSL data for each station reveal insights into the SSL and flow dynamics of the Nan River, as illustrated in Figure S1. These plots demonstrate a robust correlation between daily SSL and river flow in the upper and middle reaches, with a coefficient of determination (R^2) exceeding 0.82. Meanwhile, stations N.7A, N.8A, N.67, and C.2 displayed a moderate correlation post-1972, with R^2 values in the range of 0.6–0.7, as depicted in Figure S1e–h. Notably, in hydrological analysis, R^2 values above 0.5 are generally considered acceptable [61]. The linear regression analysis provided in Equations (8)–(17) further reveals the relationship between daily streamflow and SSL.

$$\text{Station N.64} \quad Q_s = 0.274 Q_w^{1.864} \quad R^2 = 0.82 \tag{8}$$

$$\text{Station N.1} \quad Q_s = 0.222 Q_w^{1.846} \quad R^2 = 0.84 \tag{9}$$

$$\text{Station N.13A} \quad Q_s = 0.405 Q_w^{1.602} \quad R^2 = 0.88 \tag{10}$$

$$\text{Station N.5A (from 1978 to 1997)} \quad Q_s = 0.062 Q_w^{1.946} \quad R^2 = 0.93 \tag{11}$$

$$\text{Station N.5A (from 1998 to 2019)} \quad Q_s = 0.638 Q_w^{1.424} \quad R^2 = 0.58 \tag{12}$$

$$\text{Station N.7A} \quad Q_s = 1.249 Q_w^{1.309} \quad R^2 = 0.60 \tag{13}$$

$$\text{Station N.8A} \quad Q_s = 2.656 Q_w^{1.207} \quad R^2 = 0.63 \tag{14}$$

$$\text{Station N.67} \quad Q_s = 2.684 Q_w^{1.216} \quad R^2 = 0.69 \tag{15}$$

$$\text{Station C.2 (from 1965 to 1971)} \quad Q_s = 0.026 Q_w^{2.099} \quad R^2 = 0.89 \tag{16}$$

$$\text{Station C.2 (from 1972 to 2019)} \quad Q_s = 1.221 Q_w^{1.316} \quad R^2 = 0.63 \tag{17}$$

where Q_s represents daily SSL (t/d), and Q_w represents daily streamflow (m^3/s).

3.3. Fluctuations in Anual Water Discharge and Sediment Transport along the Nan River

3.3.1. Temporal and Spatial Variation in Annual River Discharge

Results from statistical analysis and MK tests on long-term annual streamflow and annual TSL data measured during 1922–2019 are summarized in Table 3. Figure 6 depicts annual streamflow and TSL averaged over the considered periods, such as 1964–1971 (pre-construction of the Sirikit Dam), 1972–1984 (post-construction of the Sirikit Dam and pre-construction of the Naresuan Dam), 1985–2010 (post-construction of the Naresuan Dam and pre-construction of the Khwae Noi Dam), and 2011–2019 (post-construction of the Khwae Noi Dam).

Table 3 shows that the annual streamflow in the upper basin (N.64, N.1, and N.13A) varied from 1.34–13.83 $\times$ 10^9 m^3/y without a significant increasing or decreasing trend. In contrast, annual runoff in the middle basin (N.5A) ranged 3.20–15.55 $\times$ 10^9 m^3/y with a significant decreasing trend. The annual river discharges in the lower basin varied from 4.00 to 22.72 $\times$ 10^9 m^3/y with no significant trend at N.7A and N.8A, but the statistic decreasing trend was found at N.67 near the Nan basin outlet. The annual streamflow at C.2 in the CPR ranged 7.30–56.68 $\times$ 10^9 m^3/y without a statistical trend (p-values > 0.05). The results also revealed that the significantly higher discharges found at all stations occurred during flood events, such as in 1995, 2002, 2006, 2011, and 2017 (Figure 4).

Table 3. Results of the Mann–Kendall test for annual streamflow (Q_w) and estimated total sediment load (Q_t) at RID hydrological stations on the Nan River and the Chao Phraya River (significance accepted at p-value < 0.05).

Station (River)	[1] Dist. (km)	Drainage (km^2)	Data	Period	Max.	Ave.	Min.	[2] p-Value	[3] Trend
N.64	+667	3432	Q_w ($\times 10^9$ m^3/y)	1994–2019	4.568	2.599	1.338	0.294	Decreasing
(Nan)			Q_t ($\times 10^6$ t/y)		2.826	1.155	0.239	0.760	Decreasing
N.1	+635	4609	Q_w ($\times 10^9$ m^3/y)	1922–2019	6.079	2.964	1.342	0.893	Decreasing
(Nan)			Q_t ($\times 10^6$ t/y)		4.733	1.158	0.188	0.929	Decreasing
N.13A	+590	8784	Q_w ($\times 10^9$ m^3/y)	1959–2019	13.830	6.211	2.384	0.093	Increasing
(Nan)			Q_t ($\times 10^6$ t/y)		4.528	1.400	0.258	0.218	Increasing
N.5A	+223	25,286	Q_w ($\times 10^9$ m^3/y)	1951–2019	15.548	7.709	3.199	**0.027**	**Decreasing**
(Nan)			Q_t ($\times 10^6$ t/y)		6.882	1.767	0.299	**<0.0001**	**Decreasing**
N.7A	+140	29,153	Q_w ($\times 10^9$ m^3/y)	1944–2019	20.119	10.104	4.001	0.578	Decreasing
(Nan)			Q_t ($\times 10^6$ t/y)		4.176	1.261	0.344	0.087	Decreasing
N.8A	+72	31,472	Q_w ($\times 10^9$ m^3/y)	1952–2019	20.801	10.308	4.608	0.525	Decreasing
(Nan)			Q_t ($\times 10^6$ t/y)		3.833	1.239	0.254	0.564	Decreasing
N.67	+35	57,384	Q_w ($\times 10^9$ m^3/y)	1998–2019	22.725	13.185	4.264	**0.048**	**Decreasing**
(Nan)			Q_t ($\times 10^6$ t/y)		3.435	1.875	0.313	**0.021**	**Decreasing**
C.2	−5	109,973	Q_w ($\times 10^9$ m^3/y)	1956–2019	52.675	22.437	7.296	0.313	Decreasing
(CPY)			Q_t ($\times 10^6$ t/y)		21.811	4.825	0.600	**0.003**	**Decreasing**

Note: [1] Distance from the Nan River outlet: positive (+) sign is the distance from the outlet toward upstream; negative (−) sign is the distance from the outlet toward downstream; [2] p-value; [3] trends referring to the Mann-Kendall test; the statistically significant trend is marked as bold text.

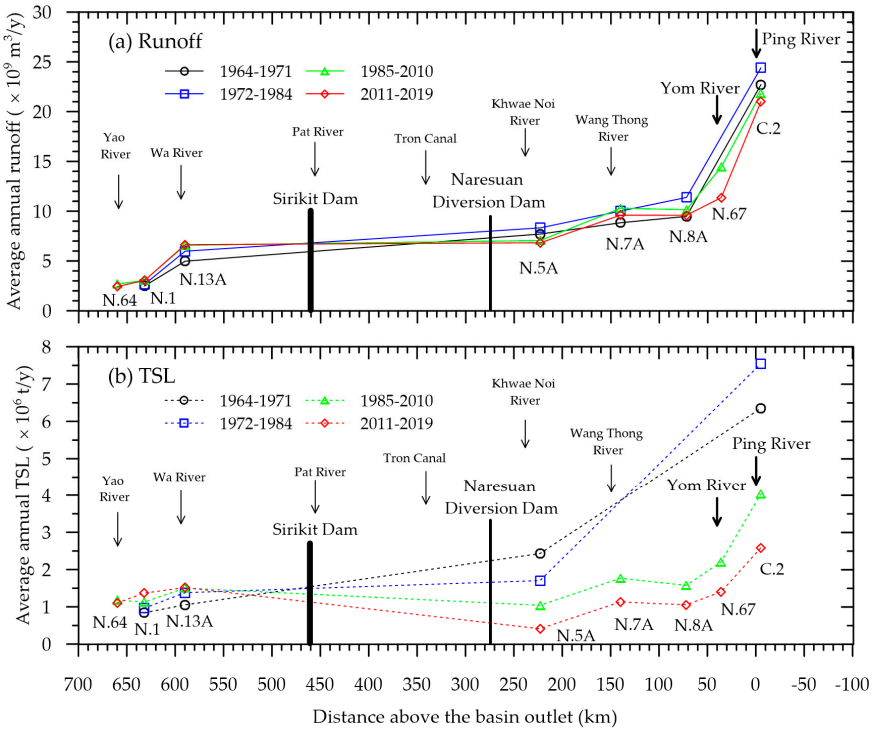

Figure 6. Results of spatial analysis at hydrological stations along the Nan River: (**a**) average annual river runoff; (**b**) average total sediment load.

The annual average river flow data (referenced in Table 3) indicates an upstream to downstream increase in the Nan River, from 2.6 × 10^9 m^3/y at the source to 13.2 × 10^9 m^3/y at the river outlet, with an average flow of 22.44 × 10^9 m^3/y recorded at C.2. Figure 6a displays the variations in average annual runoff in relation to the construction phases of key hydraulic structures such as the Sirikit Dam, the Khwae Noi Dam, and the Naresuan

diversion dam along the river. There was a notable increase in average annual runoff from upstream to downstream, as shown in Figure 6a. Additionally, the average annual runoff along the Nan River was lower before the construction of the Sirikit Dam (1963–1971) compared to the period following its construction (1972–1984). Post the establishment of the Naresuan diversion dam in 1985, the average annual runoff observed at downstream stations (N.5A, N.7A, N.8A, N.67, and C.2) after 1985 was significantly less than the pre-diversion dam period, despite an increase in flow at upstream stations (N.1 and N.13A). Figure 6a also indicates that the construction of the Khwae Noi Dam on a major Nan River tributary did not significantly impact the lower Nan River's runoff (at N.7A and N.8A). Comparing the average discharge at the Nan River basin's outlet (N.8A) with the CPR's headwater (C.2), the discharge from the Nan River contributes about 60% to overall CPR runoff, as illustrated in Figure 4.

3.3.2. Temporal and Spatial Variation in Annual TSL

The combination of SSL and BL constitutes the TSL carried by the Nan River. Assessing the variation in sediment load along the river, especially considering the impact of dam construction on sediment dynamics and contributions to the CPR system, involved estimating the TSL at each hydrological station. Due to the sporadic availability of SSL data, which was limited in both time and location, the relationship between river discharge and SSL at each station (as per Equations (8)–(17)) was applied to estimate the gaps in daily SSL data over the past decades. Subsequently, BL was inferred from these SSL estimations using the BL-to-SSL ratios derived from field surveys. For this analysis, long-term BLs at N.5A, N.7A, N.8A, and N.67 were approximated using ratios of 0.05, 0.20, 0.20, and 0.01, respectively. In the upper basin (N.64, N.1, and N.13A), BL was found to be negligible (~0). Additionally, a BL to SSL ratio of 0.03, as reported by Bidorn et al. [62], was used for estimating BL at C.2. Figure 7 presents the estimated annual TSL for the upper, middle, and lower reaches of the Nan River over the period of 1922–2019. Table 3 includes a summary of the basic statistical and trend analysis results for the annual TSL data.

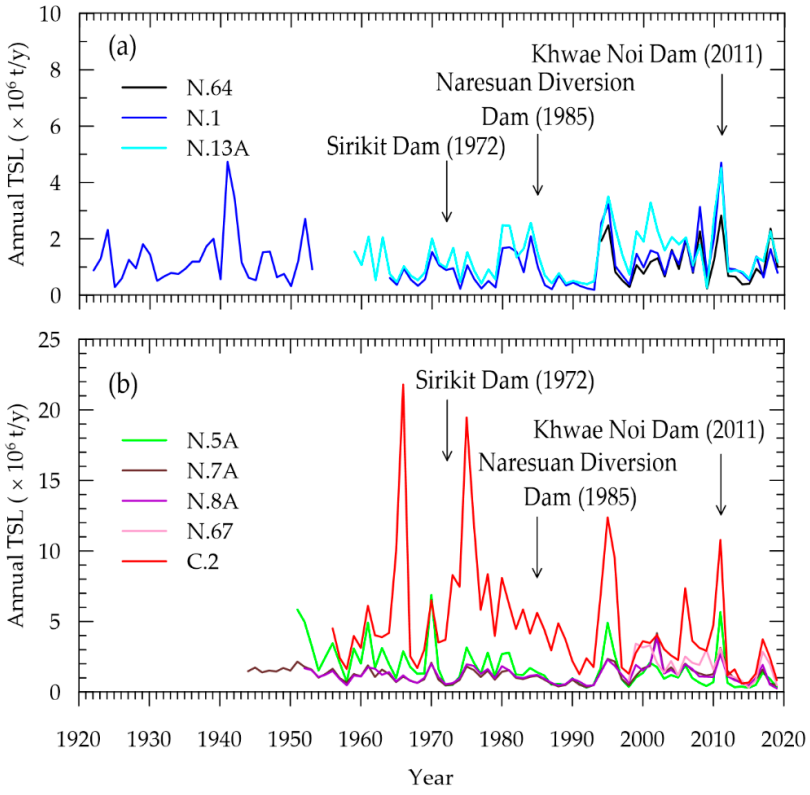

Figure 7. Annual chronological sequence of total sediment load (TSL) at RID monitoring sites from 1922 to 2019: (**a**) stations N.64, N.1, and N.13A; (**b**) stations N.5A, N.7A, N.8A, N.67, and C.2.

The Mann–Kendall test outcomes (as shown in Table 3) reveal no significant trends (with p-values < 0.05) in the annual TSL at stations N.64, N.1, N.13A, N.7A, and N.8A. However, a notable decreasing trend was observed in the annual TSL at stations N.5A and N.67 (p-values < 0.05). In terms of quantity, the upper and middle basins experienced annual TSL fluctuations between 0.19 and 4.73 $\times$ 10^6 t/y, and 0.30 to 6.88 $\times$ 10^6 t/y, respectively. For the lower basin, these values ranged from 0.25 to 4.18 $\times$ 10^6 t/y. Meanwhile, the annual TSL at station C.2 varied between 0.6 and 21.811 $\times$ 10^6 t/y, exhibiting a significant decreasing trend (p-values < 0.05). It was also noted that the annual TSLs at all stations peaked during flood years, such as those recorded in 1995, 2002, 2006, 2011, and 2017, which is depicted in Figure 7.

The spatial variation analysis of annual TSL revealed that the average long-term annual TSLs at N.64, N.1, N.13A, N.5A, N.7A, N.8A, N.67, and C.2 were 1.155, 1.158, 1.400, 1.669, 1.476, 1.372, 1.875, and 4.825 $\times$ 10^6 t/y, respectively (Table 3). Unlike the annual river discharge, the average annual TSLs after the dams' building fluctuated along the river. In the river upstream of the Sirikit Dam, the average sediment load of all time periods (1964–1971, 1972–1984, 1985–2010, and 2011–2019) increased upstream to downstream (Figure 6b). Meanwhile, the average annual TSLs downstream of the Sirikit Dam rose along the river (Figure 6b). However, the average yearly TSL of N.7A was greater than N.8A after the construction of the Naresuan Dam in 1985. Additionally, the average annual sediment load of all time periods significantly climbed at C.2 (Figure 6b). Based on Figure 6b, prior to the construction of the Sirikit and Naresuan dams, there was an observed increase in the average annual sediment load along the river from the upper to the lower reaches. The data reveal that the average annual TSLs at N.1 and N.13A, located upstream of the Sirikit Dam, were higher during 1972–2019 compared to the pre-dam construction period of 1964–1971. Furthermore, post-construction observations indicate a significant reduction in the average annual TSL at N.5A: a 30% decrease following the construction of the Sirikit Dam (1972–1984), a 57% decrease post-Naresuan Dam (1985–2010), and an 83% decrease following the Khwae Noi Dam (2011–2019). Conversely, the average annual TSL at Station C.2 exhibited an initial increase of 17% during 1972–1984, followed by reductions of 40% and 61% in the periods of 1985–2010 and 2010–2019, respectively. The sediment data reveals that the average annual TSL at N.67 between 1998 and 2019 accounted for 70% of the C.2 (Figure 7).

3.4. Influence of Major Dams on the Nan River's Discharge and Sediment Dynamics

The study utilized DMCs of cumulative annual precipitation against cumulative annual runoff, alongside cumulative annual runoff versus cumulative annual TSL, to evaluate the impact of the Sirikit, Naresuan, and Khwae Noi dams on river hydrology and sediment transport. Figures 8 and 9 display these DMCs for six stations along the Nan River, covering the period from 1944 to 2019. An analysis of Figure 8 indicates variations in the DMC slopes for stations along the Nan River (as seen in Figure 8a–e) during the period from 1975 to 1994, while a slight decrease was noted in the DMC slope at C.2 during 1985–1994. A notable change in the DMC slope across all stations occurred in 2011, coinciding with the significant flood event in Thailand that year.

Figure 9 presents DMC plots for annual runoff and TSL, showcasing the influence of the construction of three dams on the sediment dynamics in the Nan River and its contribution to the CPR. The DMC slopes for stations N.1 and N.13A (Figure 9a,b) reveal fluctuations in sediment load in the Nan River's upper reaches (upstream of the Sirikit Dam) between 1975 and 1994, in correlation with changes in river runoff. In contrast, a notable slope reduction in the DMC of N.5A (Figure 9c), situated in the middle basin (downstream of the dams), was observed post-1972, followed by a slope increase from 1975 to 1984. A subsequent decline in slope at N.5A began in 1985, coinciding with the construction of the Naresuan diversion dam. The DMCs for N.7A and N.8A in the lower basin (Figure 9d,e) exhibited minimal slope changes from 1997 to 2019. The DMC for C.2,

as depicted in Figure 9f, showed a significant slope increase from 1972 to 1995, followed by a gradual decrease after 1996.

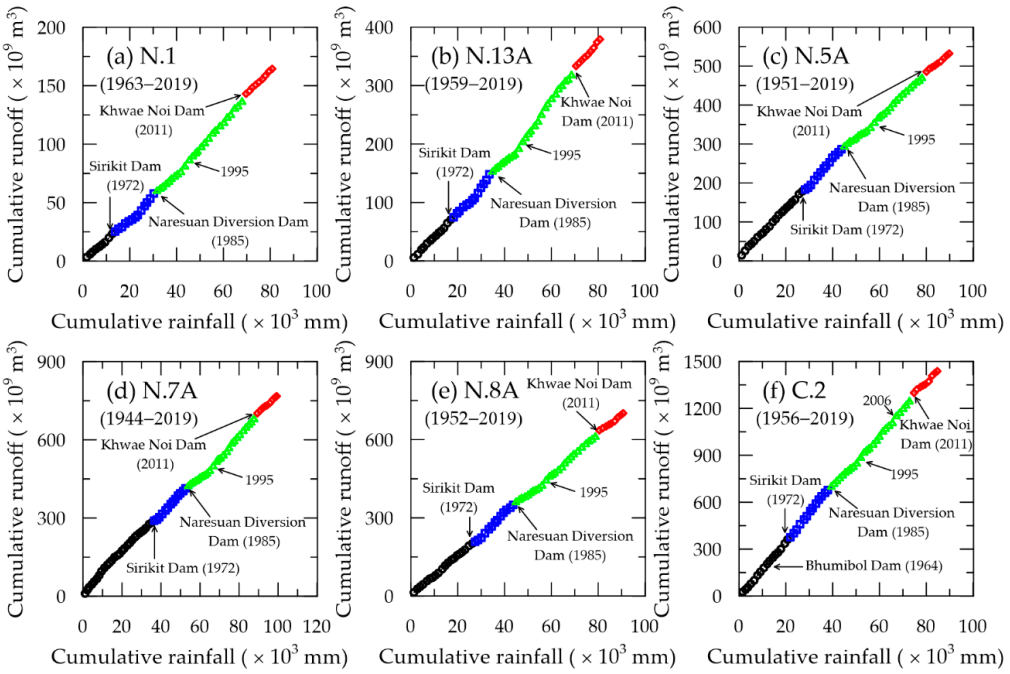

Figure 8. Double-mass curves of annual rainfall and river runoff on the Nan River: (**a**) at N.1; (**b**) at N.13A; (**c**) at N.5A; (**d**) at N.7A; (**e**) at N.8A; (**f**) at C.2. The colored points indicate various periods: black for before the construction of the Sirikit Dam, blue for before the construction of the Naresuan diversion dam, green for before the construction of the Khwae Noi Dam, and red for after the construction of the Khwae Noi Dam.

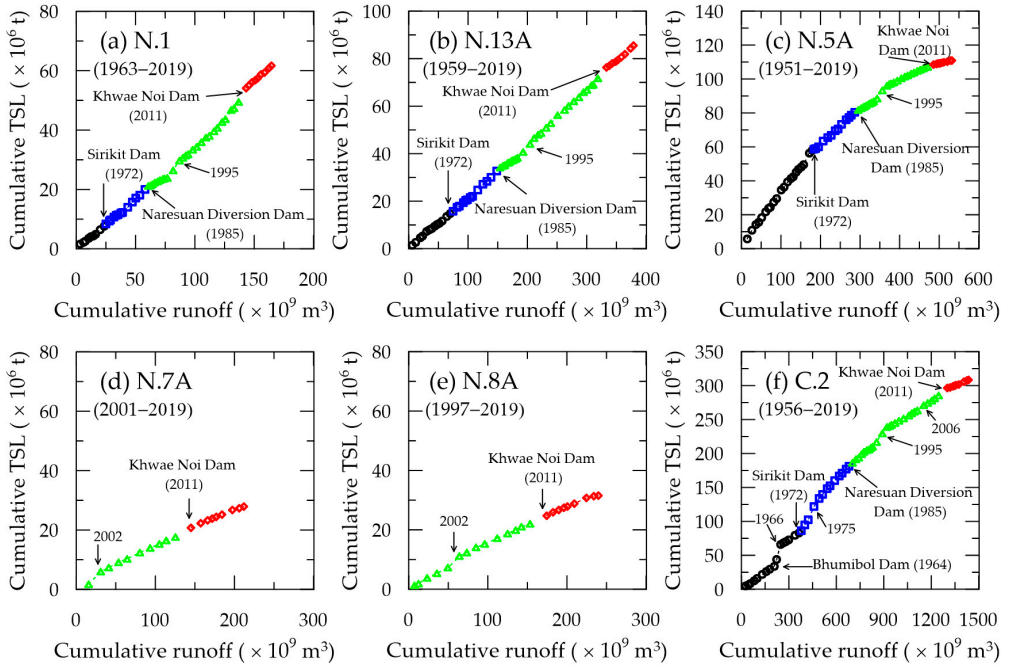

Figure 9. Double-mass curves of annual runoff and total sediment load (TSL) on the Nan River: (**a**) at N.1; (**b**) at N.13A; (**c**) at N.5A; (**d**) at N.7A; (**e**) at N.8A; (**f**) at C.2. The color coding indicates different phases: black for the period before the Sirikit Dam construction, blue for before the Naresuan diversion dam construction, green for before the Khwae Noi Dam construction, and red for after the Khwae Noi Dam was built.

4. Discussion

4.1. Sediment Dynamics in the Nan River

Among the four primary tributaries (the Ping, Wang, Yom, and Nan rivers) that constitute the CPR, the sediment transport dynamics of the Nan River have not been extensively researched or detailed in the literature [38]. Based on the observed sediment data in 2018 (Table 2), the upper Nan River (gradient 1:3000) contained coarse sand to fine gravel, the middle reach (gradient less than 1:5000) had fine to very coarse sand, and the lower reach (1:14,300) comprised medium to coarse sand. Although all tributaries of the upper CPR basin are neighboring and similar in terms of climate [12,25,63], the bed materials of each river were different. The composition of the Nan River's riverbed sediment, characterized by larger particles compared to other tributaries, may be affected by the operations of the Sirikit, Naresuan, and Khwae Noi dams. The release of clear water from these dams could have the capacity to transport finer sediments downstream, leaving behind the coarser sediment on the riverbed.

The TSL of the Nan River primarily consists of suspended sediments, mirroring the sediment characteristics of the Yom River, yet differing from those of the Ping and Wang rivers. Post-Bhumibol Dam, the Ping River's SSL varies from 2% to 70% of its TSL [12]. Following the construction of the Kiew Koh Ma and Kiew Lom dams, the Wang River sees its SSL contributing 20% to 22% of the TSL [25]. In contrast, beneath the Sirikit Dam, the Nan River's SSL accounts for a much larger portion, ranging between 72% and 100% of the TSL. This higher proportion is largely due to the sediment retention by the Sirikit Dam and the build-up upstream of the Naresuan diversion dam. Downstream of this diversion dam, the river's diminished flow lessens its capacity to carry bed sediment, resulting in an increase in SSL. This increase in SSL is attributed to finer sediment contributions from major tributaries such as the Pat River, Tron Canal, Khwae Noi River, Wang Thong River, and Yom River, in addition to runoff from adjacent agricultural lands (illustrated in Figure 1b). This surge, along with altered flow patterns, weakens the correlation between daily SSL and river discharge in the lower reaches of the Nan River and the CPR (at stations N.5A, N.7A, N.8A, N.67, and C.2), as shown in Figure S1. The moderate correlation seen between daily SSL and discharge is influenced by the lower flow velocities, a result of the reduced river gradient shown in Figure 2, leading to pronounced sedimentation in these lower sections [46]. A similar trend of weak correlation between daily SSL and runoff is also noted in the lower Yom River [37] and the lower reaches of the Yangtze River [17].

In rivers with gentler gradients (less steep than 1:500), BL usually comprises approximately 10–20% of the TSL, whereas rivers with steeper gradients (exceeding 1:500) often see BL contributing about 20–30% [64]. In Thailand's river systems, the RID generally estimates BL at around 30% of the SSL, which translates to nearly 23% of the TSL for various hydro projects [65]. The Nan River, classified as non-mountainous due to its gradient (as illustrated in Figure 2), presents a different scenario with BL percentages in its upper, middle, and lower reaches at 0–0.2%, 0–9.7%, and 0.1–27.6% of the TSL, respectively. These proportions are atypical when compared to traditional estimates, likely influenced by dam regulation and water management initiatives [64]. BL is notably lower in the upper Nan basin, as the TSL is predominantly comprised of suspended sediments, including significant wash load components within the SSL.

The riverbed slope transition from 1:500 to 1:3000 leads to a decrease in flow velocity and sediment carrying capacity, resulting in increased sediment deposition [45]. Smaller dams upstream may also be intercepting BL from tributaries [38]. This pattern of reduced BL is consistent with findings from the upper stretches of the Ping, Wang, and Yom rivers [12,25,37]. Conversely, BL in the middle and lower stretches of the Nan River is elevated due to the effects of dam activities. For example, BL downstream of the Bhumibol Dam on the Ping River accounts for more than 80% of the TSL [12], while the Wang River experiences BL constituting 78–80% of the TSL after the Kiew Koh Ma and Kiew Lom dams [25]. In the Yom River, which lacks large-scale dams, the BL proportion in its middle and lower sections remains below 5% of the TSL [37].

The study underscores the marked variability in sediment characteristics across different rivers and within various segments of the same river, illustrating their unique area-specific nature. It is imperative that continual and detailed monitoring is carried out to obtain accurate sediment data, which is indispensable for informed water resource management and sustainable development planning.

4.2. Hydrological and Sediment Transport Patterns in the Nan River Basin

Environmental conditions and anthropogenic influences, notably precipitation, are key determinants of variations in runoff and sediment loads [19,22,66]. Analysis using the Mann–Kendall (MK) statistical approach for the upper Nan River basin's streamflow data indicated an absence of a significant trend in annual runoff, with *p*-values exceeding 0.05. This indicates the predominance of climatic elements, with a particular emphasis on rainfall, as the primary drivers of discharge fluctuations [8,11,55]. However, a declining trend in streamflow was observed in the middle reach at station N.5A (p-value = 0.027), likely due to the Naresuan diversion dam's impacts, as evidenced by the reduction in the DMC of cumulative rainfall and discharge between 1985 and 2011 (Figure 8c). In the lower river, no significant streamflow decrease was found at stations N.7A, N.8A, and C.2, although the DMCs indicated a decreased slope after 1985 and 2011 (Figure 8d–f). This also suggests the Naresuan diversion dam may have influenced the lower-reach flow reduction, while tributaries and irrigation canals might have compensated for the runoff. Additionally, station N.67 showed a significant decline trend in streamflow (MK test, p-value = 0.048), reflecting the Naresuan diversion dam's impact. High streamflow during flood years (1966, 1975, 1995, 2002, 2006, 2011, and 2017) contrasted with a declining trend in 1981–1993 across all stations, mirroring a low-water period in Thailand [37].

Analysis of average daily water discharge and yearly runoff at various stations showed an increase in discharge downstream along the Nan River, correlating with catchment area expansion. From 1972–1984, post-Sirikit Dam and pre-Naresuan Dam, annual streamflow increased more than in the 1964–1971 pre-Sirikit Dam period, attributed to increased rainfall [56]. However, post-1985 and post-Naresuan Dam, average annual discharge upstream of the Sirikit Dam continued to rise, while it decreased downstream due to the Naresuan and Khwae Noi dams' operations. The impact of the Khwae Noi Dam on streamflow was minimal, as storage dams typically release yearly discharge downstream close to natural conditions (Figure S2a,c). Notably, yearly runoff at station N.7A exceeded that at N.8A after 1985, likely due to side flow from irrigation canals and the Wang Thong River (Figures 6a and S3).

Sediment studies (referenced in Table 3 and depicted in Figure 7a) show a stable trend in the TSL within the upper segment of the Nan River basin, in alignment with streamflow behavior (MK test, p-value > 0.05). The DMCs for the cumulative annual runoff against the TSL at stations N.1 and N.13A do not indicate significant shifts from 1922 to 2019 (as illustrated in Figure 9a,b), suggesting a correlation between TSL fluctuations and river discharge rates. The middle section of the river at station N.5A, however, has experienced a noticeable reduction in the annual TSL (MK test, p-value < 0.0001), with significant slope changes in the DMCs post-1985 (shown in Figure 9c), a trend that can be tied to the operations of the Naresuan diversion dam initiated in 1985 and subsequent flood control measures introduced post-1995. Further downstream, stations N.7A, N.8A, and N.67 in the lower basin registered a marked decrease in TSL (p-value < 0.05). In contrast, the data from station C.2 in the Chao Phraya River basin present a notable decline in the TSL, despite spikes during flooding events in years such as 1995, 2002, 2006, and 2011 (Figure 7). The construction of dams across the Ping, Wang, and Nan rivers has not significantly impacted sediment discharge at the mouth of these rivers, implying that the observed sediment reduction at C.2 over recent decades might stem from changes in the sediment transport pattern due to intensive water management for irrigation [31,44,62].

The spatial analysis of sediment transport patterns shows a progressive increase in the average annual TSL from upstream to downstream along the upper Nan River course

(depicted in Figure 6b), a pattern that is consistent with the sediment dynamics observed in the upper Ping River [12] and the upper Yangtze River [8]. After the construction of the Sirikit Dam in 1985, TSL variations were noted, with an increase in the lower Nan River region (N.7A) likely due to sediment contributions from irrigation channels and the Wang Thong River, as shown in Figure S3. Conversely, a reduction in TSL was observed at N.8A, indicating a zone of sediment deposition. The Marine Department's dredging activities, removing 200,000 to 700,000 m^3/y, are also contributing factors to the TSL decline in the downstream sections [12,45]. However, an increase in TSL at station N.67 suggests the influence of sediment from the Yom River, surrounding farmlands, and drainage systems. At station C.2, within the CPR basin, there was a significant rise in TSL, likely due to sediment inflows from the Nan, Yom, and Ping rivers (as indicated in Figure 6b).

4.3. Implications of Major Dams on Hydrology and Sediment Process in the Nan River

Large dams' influence on river flow and sediment dynamics has been extensively documented [3,10,24,35,67–69], such as the notable reduction in sediment delivery by the Three Gorges Dam to the Yangtze River, impacting its delta [5,8,17,22,41]. In the Chao Phraya River basin, which comprises the Ping, Wang, Yom, and Nan rivers, research has focused on sediment transport and its link to coastal erosion in the upper Gulf of Thailand [12,25,31–36]. Yet, studies indicated that the Bhumibol Dam on the Ping River and other dams in the Wang River basin, as well as the barrage on the Yom River, did not significantly alter their streamflow or sediment transport [12,25,37].

This research identified that the Sirikit Dam on the Nan River, completed in 1972, had no discernible effect on the annual water discharge, but the Naresuan diversion dam did, as reflected by the downward shift in the DMC for annual precipitation against runoff after 1985 (seen in Figure 8c–e) [38,40]. The discharge from the Naresuan diversion dam into the Nan River fluctuated, comprising 43–77% of the incoming flow, thereby affecting the volume of water withdrawn from the river [38]. The operational impact of large storage dams on the annual flow appeared minimal, aimed at maintaining ecological balance downstream [70].

Moreover, the investigation observed a reduction in TSL downstream of the Sirikit Dam subsequent to the construction of the three dams. This was attributed to sediment retention within the dam reservoirs and its diversion for irrigation use, resulting in increased sediment deposition upstream of the diversion dam (as illustrated in Figure 9c–e) [26,71]. Nonetheless, sediment load in the lower reaches of the Nan River saw an increase due to agricultural runoff and inputs from tributaries and irrigation channels, with sediment losses from rice fields approximated at 4.32×10^6 t/y [38,72]. Furthermore, the transit of bedload sediment downstream of these dams played a role in altering fluvial dynamics (as detailed in Table 2).

4.4. Consequences of Large Dams on River Discharge and Sediment Supply to the Chao Phraya River

The streamflow and sediment supply into the CPR system were assessed at station C.2, summarizing the Ping and Nan rivers' contributions. C.2's average annual streamflow was 22.473×10^9 m^3/year with no trend, while its TSL significantly decreased to 4.83×10^6 t/y, particularly after the construction of three large dams in the Nan River basin (Figure 7, Table 3). Annual river discharge and TSL data (1954–2019) at P.17 (Ping River), N.67 (Nan River), and C.2 showed that river discharge at N.67 and P.17 contributed 60% and 35% to C.2's runoff, respectively (Figure 10a). The Yom River (Y.16) contributed about 33% to N.67's discharge, equating to 20% of C.2's flow, while the Wang River basin provided about 15% and 5% to P.17's and C.2's runoff, respectively [25,37]. The Nan (N.67) and Ping (P.17) Rivers accounted for 70% and 26% of the CPR's annual TSL at C.2 (Figure 10b). The sediment concentration was higher in the Nan River, especially during the wet season (Figures S4 and S5). Therefore, the Nan River basin emerged as the largest contributor of both water (40%) and sediment (57%) to the CPR system.

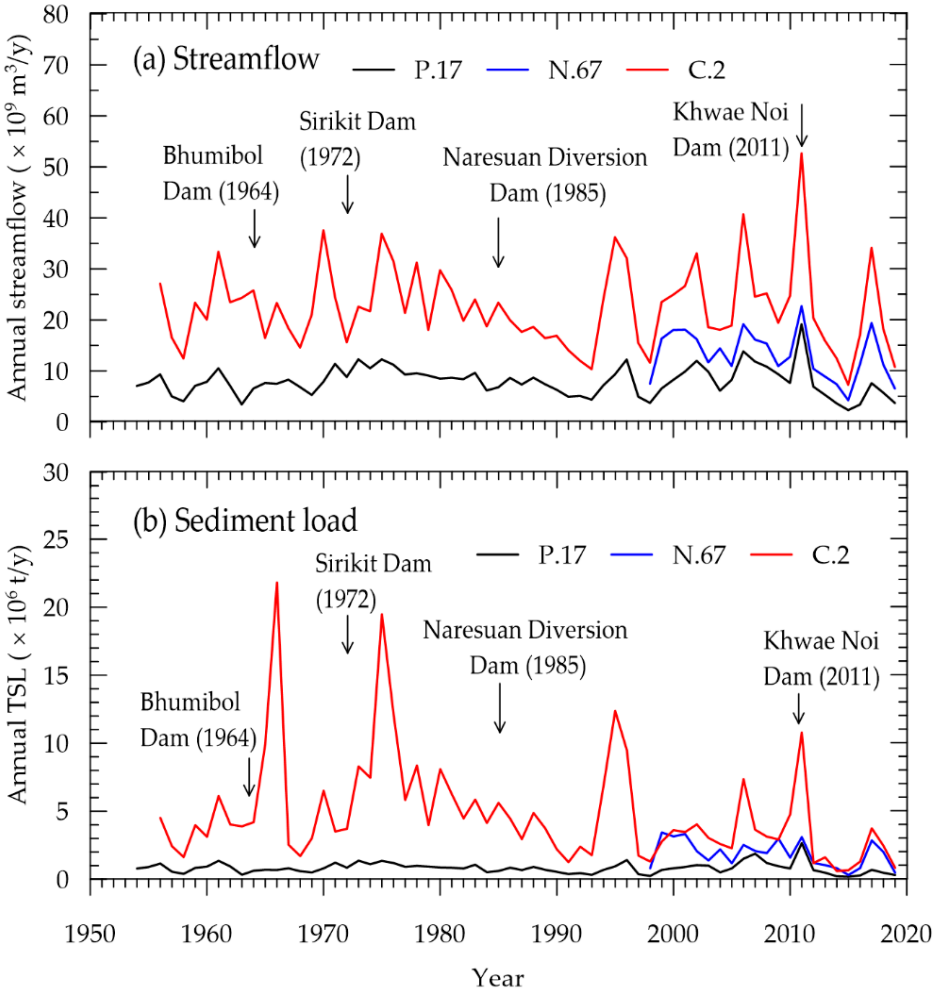

Figure 10. Chronological sequence of (**a**) annual streamflow and (**b**) annual TSL at RID Stations P.17, N.67, and C.2 from 1954 to 2019.

As evidenced by the diminishing slope of the cumulative annual rainfall and runoff DMC at station C.2 (Figure 8f), the construction of the Naresuan and Khwae Noi dams likely led to a decreased annual streamflow in the CPR post-1985 and 2011. This was primarily due to the diversion of the Nan River's flow for irrigation by the Naresuan Dam (Figure S2b) and water allocation for irrigation from the Khwae Noi Dam [40]. These developments also obviously reduced the annual TSL in the CPR, indicated by a lower DMC slope post-1985 and 2011 (Figure 9f). In contrast, increased TSL at C.2 was found after the construction of the Sirikit Dam in 1972 (Figure 9f). Despite trapping upstream sediment, the downstream expansion of agriculture [38,43] and intensified rice cultivation in the Nan River basin (2–3 crops/y) [72] led to an increased sediment load of approximately 4.32×10^6 t/y. These factors, along with river cross-section improvements by the RID in the lower Nan River during 1973–1975 [73], contributed to an enhanced sediment load after 1972.

The remote location of the Sirikit Dam from C.2 (465 km) meant its impact on the TSL and streamflow at C.2 was minimal. The Kiew Lom Dam on the Wang River also had little effect on TSL at the river basin outlet due to its downstream agricultural expansion [25]. Conversely, the Bhumibol Dam slightly reduced TSL after 1966 (Figure 9f) due to sediment trapping, with increased sediment yield downstream from expanded irrigation (approximately 97,600 ha). Soil loss from agricultural activities in the lower Ping River basin added approximately 2.135×10^6 t/y of sediment (Figure 9f) [72]. The TSL increase

during 1964–1966 was influenced by the RID's river enhancements and agricultural growth following the Bhumibol Dam's construction [73].

The research identified a marked decline in the DMC slope at station C.2 after 1995, a trend linked to the construction of a new hydraulic infrastructure for flood management and agricultural water distribution in the lower basins of the Ping, Yom, and Nan rivers. This was further influenced by intensive dredging activities in the lower Nan River, downstream from station N.67, where an estimated 360,000 to 1,260,000 t of sediment were extracted annually [25,45] (as indicated in Figure 9f). The increased channel cross-section resulting from this dredging led to slower flow rates and sediment conveyance, causing an accumulation of sediment upstream of the CPR. It is well documented that major dams retain a large portion of upstream sediments [74], thus diminishing the TSL further downstream. However, their impact is also critical in modulating sediment discharge at the outlets of river basins. Post-construction of the Sirikit and Bhumibol dams, there was a surge in TSL at C.2, which contrasts with the subsequent decline following the establishment of the Khwae Noi Dam and other flood mitigation measures, mirroring the sediment-reduction trends seen in major rivers such as the Yangtze [8], Yellow [55], and Nile [23] due to damming. Compared to earlier studies at C.2, this analysis found only a 31% reduction in CPR sediment load post-2011, as opposed to the 75–85% reduction observed in the pre-1995 period, before the construction of these mega-dams [33–36,47] (Figure 9f).

5. Conclusions

In this study, we examined sediment characteristics, streamflow variation, and the impact of three large dams in the Nan River basin on the runoff and sediment load in the Nan River and the Chao Phraya River at C.2. Our findings indicate that the Nan River is a significant contributor to the CPR, providing 40% of the water outflow and 57% of the TSL. The river, primarily an alluvial system with fine sand to very fine gravel, transports most sediment in suspension. Notably, the Naresuan diversion dam obviously led to a decrease in both runoff and TSL in the Nan River, particularly downstream, while the Sirikit Dam primarily reduced TSL. Post-construction of the Bhumibol and Sirikit dams, the total sediment load at C.2 increased due to expanded irrigation and agricultural activities downstream, contrasting with the decline after 1985 due to intensive water regulation in the upper CPR basin. The sediment load at C.2 decreased by only 31% post-dam construction compared to the pre-dam period (1956–1963). These findings highlight the complex impact of dam construction on river basin sediment dynamics, illustrating how dams aimed at irrigation expansion can increase sediment load, while those for flood control and water use can decrease it. Additionally, this study underscores the need for integrated approaches in sustainable food and water management in the CPR basin. Considering the environmental challenges posed by large-scale reservoir projects, our insights emphasize the importance of balancing agricultural productivity with environmental conservation. Future efforts should focus on optimizing water-use efficiency, promoting eco-friendly agricultural practices, and enhancing sediment management strategies to ensure the long-term sustainability and resilience of food and water resources in the region.

Supplementary Materials: The following are available online at https://www.mdpi.com/article/10.3390/w16010148/s1, Figure S1: Sediment rating curves at eight RID hydrological stations: (a) N.64; (b) N.1; (c) N.13A; (d) N.5A; (e) N.7A; (f) N.8A; (g) N.67; (h) C.2; Figure S2: Annual inflow and outflow of dams (a) Sirikit Dam; (b) Naresuan Diversion Dam; (c) Khwae Noi Dam; Figure S3: The streamflow and sediment supply into the middle and lower reaches of the Nan River from the tributaries and drainage canals; Figure S4: Comparison between the concentration of sediment in the Ping and Nan rivers: (a) 1985; (b) 2003; (c) 2010; (d) 2014; (e) 2017; (f) 2020; and Figure S5: Comparison between the sediment concentration in the Yom and Nan rivers: (a) 2008; (b) 2010; (c) 2014; (d) 2017; (e) 2018; (f) 2020.

Author Contributions: Conceptualization, M.N. and B.B.; methodology, M.N. and R.M.; formal analysis, M.N., B.B. and R.M.; investigation, B.B., M.N. and W.C.; resources, R.M.; data curation, M.N. and R.M.; writing—original draft preparation, M.N.; writing—review and editing, B.B.; visualization, M.N. and W.C.; supervision, B.B.; project administration, B.B.; funding acquisition, B.B. All authors have read and agreed to the published version of the manuscript.

Funding: This research was funded by Chulalongkorn University, grant number GB-B_62_011_21_05 and the Office of the Higher Education Policy, Science, Research, and Innovation National Council (NRCT) by the Human Resource Development and Management Unit and Funding for the Development of Higher Education Institutions Research and Innovation Creation, grant number B05F630024.

Data Availability Statement: The data presented in this study is available on request from the corresponding author.

Acknowledgments: The authors acknowledge the support of the RID for providing the river datasets used in this study. The authors also acknowledge the support of the 100th Anniversary Chulalongkorn University Fund for Doctoral Scholarship, the 90th Anniversary Chulalongkorn University Fund (Ratchadaphiseksomphot Endowment Fund: GCUGR1125633037D).

Conflicts of Interest: The authors declare no conflicts of interest.

References

1. Peng, J.; Chen, S.L.; Dong, P. Temporal variation of sediment load in the Yellow River basin. *CATENA* **2010**, *2*, 135–147. [CrossRef]
2. Charoenlerkthawin, W.; Bidorn, K.; Panneerselvam, B.; Sriariyawat, A.; Otarawanna, S.; Bidorn, B. Monitoring of nature-based solution for stabilizing eroded muddy coastline of the Chao Phraya Delta, Thailand. *IOP Conf. Ser. Earth Environ. Sci.* **2023**, *1226*, 012013. [CrossRef]
3. Liu, S.W.; Zhang, X.F.; Xu, Q.X.; Liu, D.C.; Yuan, J.; Wang, M.L. Variation and driving factors of water discharge and sediment load in different regions of the Jinsha River basin in China in the past 50 years. *Water* **2019**, *11*, 1109. [CrossRef]
4. Das, S. Dynamics of streamflow and sediment load in Peninsular India rivers. *Sci. Total Environ.* **2021**, *799*, 149372. [CrossRef] [PubMed]
5. Zhang, X.; Dong, Z.; Gupta, H.; Wu, G.; Li, D. Impact of the Three Gorges Dam on the hydrology and ecology of the Yangtze River. *Water* **2016**, *8*, 590. [CrossRef]
6. Liu, C.; He, Y.; Li, Z.; Chen, J.; Li, Z. Key drivers of changes in the sediment loads of Chinese rivers discharging to the oceans. *Int. J. Sediment Res.* **2021**, *36*, 747–755. [CrossRef]
7. Guo, P.; Geissen, V.; Ritsema, C.J.; Mu, X.M.; Wang, F. Impact of climate change and anthropogenic activities on streamflow and sediment discharge in the Wei River basin, China. *Hydrol. Earth Syst. Sci.* **2013**, *17*, 961–972. [CrossRef]
8. Zhao, Y.; Zou, X.; Liu, Q.; Yao, Y.; Li, Y.; Wu, X.; Wang, C.; Yu, W.; Wang, T. Assessing natural and anthropogenic influences on water discharge and sediment load in the Yangtze River, China. *Sci. Total Environ.* **2017**, *607–608*, 920–932. [CrossRef]
9. Charoenlerkthawin, W.; Bidorn, K.; Otarawanna, S.; Bidorn, B. Effect of Coastal Protection Structures on Beach Material Transformation. In Proceedings of the 40th IAHR World Congress, Rivers–Connecting Mountains and Coasts (IAHR 2023), Vienna, Austria, 21–25 August 2023; pp. 517–523. [CrossRef]
10. Walling, D.E. Human impact on land-ocean sediment transfer by the world's rivers. *Geomorphology* **2006**, *79*, 192–216. [CrossRef]
11. Jiang, C.; Zhang, L.; Li, D.; Li, F. Water discharge and sediment load changes in China: Change patterns, causes, and implications. *Water* **2015**, *7*, 5849–5875. [CrossRef]
12. Namsai, M.; Charoenlerkthawin, W.; Sirapojanakul, S.; Burnett, W.C.; Bidorn, B. Did the construction of the Bhumibol Dam cause a dramatic reduction in sediment supply to the Chao Phraya River? *Water* **2021**, *13*, 386. [CrossRef]
13. Tessler, Z.D.; Vörösmarty, C.J.; Grossberg, M.; Gladkova, I.; Aizenman, H.; Syvitski, J.P.M.; Georgiou, E.F. Profiling risk and sustainability in coastal deltas of the world. *Science* **2015**, *349*, 638–643. [CrossRef] [PubMed]
14. Bidorn, B.; Sok, K.; Bidorn, K.; Burnett, W.C. An analysis of the factors responsible for the shoreline retreat of the Chao Phraya Delta (Thailand). *Sci. Total Environ.* **2021**, *769*, 145253. [CrossRef] [PubMed]
15. Lu, X.X.; Oeurng, C.; Le, T.P.Q.; Thuy, D.T. Sediment budget as affected by construction of a sequence of dams in the lower Red River, Vietnam. *Geomorphology* **2015**, *248*, 125–133. [CrossRef]
16. Guo, L.; Su, N.; Zhu, C.; He, Q. How have the river discharges and sediment loads changed in the Changjiang River Basin downstream of the Three Gorges Dam? *J. Hydrol.* **2018**, *560*, 259–274. [CrossRef]
17. Yang, H.F.; Yang, S.L.; Xu, K.H.; Milliman, J.D.; Wang, H.; Yang, Z.; Chen, Z.; Zhang, C.Y. Human impacts on sediment in the Yangtze River: A review and new perspectives. *Glob. Planet. Chang.* **2018**, *162*, 8–17. [CrossRef]
18. Binh, V.D.; Kantoush, S.; Sumi, T. Changes to long-term discharge and sediment loads in the Vietnamese Mekong Delta caused by upstream dams. *Geomorphology* **2020**, *353*, 107011. [CrossRef]
19. Guo, C.; Jin, Z.; Guo, L.; Lu, J.; Ren, S.; Zhou, Y. On the cumulative dam impact in the upper Changjiang River: Streamflow and sediment load changes. *CATENA* **2020**, *184*, 104250. [CrossRef]

20. Reisenbüchler, M.; Bui, M.D.; Rutschmann, P. Reservoir sediment management using artificial neural networks: A case study of the lower section of the Alpine Saalach River. *Water* **2021**, *13*, 818. [CrossRef]
21. Ve, N.D.; Fan, D.; Van Vuong, B.; Lan, T.D. Sediment budget and morphological change in the Red River Delta under increasing human interferences. *Mar. Geol.* **2021**, *431*, 106379. [CrossRef]
22. Tian, Q.; Xu, K.H.; Dong, C.M.; Yang, S.L.; He, Y.J.; Shi, B.W. Declining sediment discharge in the Yangtze River from 1956 to 2017: Spatial and temporal changes and their causes. *Water Resour. Res.* **2021**, *57*, e2020WR028645. [CrossRef]
23. Shalash, S. Effects of sedimentation on the storage capacity of the High Aswan Dam reservoir. *Hydrobiologia* **1982**, *91*, 623–639. [CrossRef]
24. Wu, Z.; Zhao, D.; Syvitski, J.P.M.; Saito, Y.; Zhou, J.; Wang, M. Anthropogenic impacts on the decreasing sediment loads of nine major rivers in China, 1954–2015. *Sci. Total Environ.* **2020**, *739*, 139653. [CrossRef] [PubMed]
25. Charoenlerkthawin, W.; Namsai, M.; Bidorn, K.; Rukvichai, C.; Panneerselvam, B.; Bidorn, B. Effects of dam construction in the Wang River on sediment regimes in the Chao Phraya River basin. *Water* **2021**, *13*, 2146. [CrossRef]
26. Chong, X.Y.; Vericat, D.; Batalla, R.J.; Teo, F.Y.; Lee, K.S.P.; Gibbins, C.N. A review of the impacts of dams on the hydromorphology of tropical rivers. *Sci. Total Environ.* **2021**, *794*, 148686. [CrossRef] [PubMed]
27. Bidorn, B.; Phanomphongphaisarn, N.; Rukvichai, C.; Kongsawadworakul, P. Evolution of mangrove muddy coast in the Western Coast of the Upper Gulf of Thailand over the past six decades. In *Estuaries and Coastal Zones in Times of Global Change*; Nguyen, K., Guillou, S., Gourbesville, P., Thiébot, J., Eds.; Springer: Singapore, 2020; pp. 429–442.
28. Vongvissessomjai, S. Chao Phraya Delta: Paddy field irrigation areas in tidal deposits. In Proceedings of the 56th International Executive Council of ICID, Beijing, China, 10–18 September 2005. Available online: https://www.rid.go.th/thaicid/_5_article/2549/10_1ChaoPhraYaDelta.pdf (accessed on 13 April 2021).
29. Tanabe, S.; Saito, Y.; Sato, Y.; Suzuki, Y.; Sinsakul, S.; Tiyapairach, S.; Chaimanee, N. Stratigraphy and Holocene evolution of the mud-dominated Chao Phraya delta, Thailand. *Quat. Sci. Rev.* **2003**, *22*, 789–807. [CrossRef]
30. Chen, G.; Xu, B.; Bidorn, B.; Burnett, W.C. Effects of Groundwater Extraction and River Regulation on Coastal Freshwater Resources. In *Blue Economy: An Ocean Science Perspective*; Urban, E.R., Jr., Ittekkot, V., Eds.; Springer: Singapore, 2022; pp. 123–152.
31. Charoenlerkthawin, W.; Bidorn, K.; Burnett, W.C.; Sasaki, J.; Panneerselvam, B.; Bidorn, B. Effectiveness of grey and green engineered solutions for protecting the low-lying muddy coast of the Chao Phraya Delta, Thailand. *Sci. Rep.* **2022**, *12*, 20448. [CrossRef]
32. Burnett, W.C.; Bidorn, B.; Wang, Y. Can 210Pb be used as a paleo-storm proxy? *Quat. Sci. Rev.* **2023**, *315*, 108242. [CrossRef]
33. Winterwerp, J.C.; Borst, W.G.; De Vries, M.B. Pilot study on the erosion and rehabilitation of a mangrove mud coast. *J. Coast. Res.* **2005**, *21*, 223–230. [CrossRef]
34. Uehara, K.; Sojisuporn, P.; Saito, Y.; Jarupongsakul, T. Erosion and accretion processes in a muddy dissipative coast, the Chao Phraya River delta, Thailand. *Earth Surf. Process. Landf.* **2010**, *35*, 1701–1711. [CrossRef]
35. Milliman, J.D.; Farnsworth, K.L. *River Discharge to the Coastal Ocean: A Global Synthesis*; Cambridge University Press: New York, NY, USA, 2011; pp. 1–382.
36. Gupta, H.; Kao, S.J.; Dai, M. The role of mega dams in reducing sediment fluxes: A case study of large Asian rivers. *J. Hydrol.* **2012**, *464–465*, 447–458. [CrossRef]
37. Namsai, M.; Bidorn, B.; Chanyotha, S.; Mama, R.; Phanomphongphaisarn, N. Sediment dynamics and temporal variation of runoff in the Yom River, Thailand. *Int. J. Sediment Res.* **2020**, *35*, 365–376. [CrossRef]
38. Hydro and Agro Informatics Institute (HAII). *Report on Data Collection and Analysis: Database Development Project and Flood and Drought Modeling of 25 River Basins (Nan River Basin)*; Hydro and Agro Informatics Institute: Bangkok, Thailand, 2012. (In Thai)
39. Japan International Cooperation Agency (JICA). *Project for the Comprehensive Flood Management Plan for the Chao Phraya River Basin*; Final Report; Office of National Economic and Social Development Board: Bangkok, Thailand, 2013.
40. Royal Irrigation Department (RID). *A Study of Dam Break Project of Khwae Noi Dam, Phitsanulok Province*; Royal Irrigation Department: Bangkok, Thailand, 2009. (In Thai)
41. Wang, Y.; Rhoads, B.L.; Wang, D.; Wu, J.; Zhang, X. Impacts of large dams on the complexity of suspended sediment dynamics in the Yangtze River. *J. Hydrol.* **2018**, *558*, 184–195. [CrossRef]
42. Royal Irrigation Department (RID). *Nan River Basin Hydrometeorological Report*; Royal Irrigation Department: Bangkok, Thailand, 1969.
43. Bidorn, B.; Namsai, M.; Charoenlerkthawin, W.; Bidorn, K. Recent Changes in Sediment Supply to the Chao Phraya Delta. In Proceedings of the 40th IAHR World Congress, Rivers–Connecting Mountains and Coasts (IAHR 2023), Vienna, Austria, 21–25 August 2023; pp. 16–25. [CrossRef]
44. Office of Natural Resources and Environmental Policy and Planning (ONEP). *Developing Watershed Management Organizations in Pilot Sub-Basins of the Ping River Basin*; Final Report; Office of Natural Resources and Environmental Policy and Planning, Ministry of Natural Resources and Environment: Bangkok, Thailand, 2005. (In Thai)
45. Marine Department (MD). *The Feasibility Study of River Navigation, Port, Revetment for Rivers in the North and North-East of Thailand: Nan River*; Marine Department: Bangkok, Thailand, 2002. (In Thai)
46. Electricity Generating Authority of Thailand (EGAT). *Sediment Survey of Sirikit Dam*; Report No. 31303-3603; Electricity Generating Authority of Thailand: Bangkok, Thailand, 1993.
47. Japan International Cooperation Agency (JICA). *The Feasibility Study on Mangrove Revival and Extension Project in the Kingdom of Thailand*; Final Report; Ministry of Agriculture: Bangkok, Thailand, 2001.

48. Edwards, T.K.; Glysson, G.D.; Guy, H.P.; Norman, V.W. *Field Methods for Measurement of Fluvial Sediment*; US Geological Survey: Denver, CO, USA, 1999; pp. 1–89.
49. Helley, E.J.; Smith, W. *Development and Calibration of a Pressure-Difference Bedload Sampler*; US Department of the Interior, Geological Survey, Water Resources Division: Menlo Park, CA, USA, 1971; pp. 1–18.
50. Lemma, H.; Nyssen, J.; Frankl, A.; Poesen, J.; Adgo, E.; Billi, P. Bedload transport measurements in the Gilgel Abay River, Lake Tana Basin, Ethiopia. *J. Hydrol.* **2019**, *577*, 123968. [CrossRef]
51. Rachlewicz, G.; Zwoliński, Z.; Kociuba, W.; Stawska, M. Field testing of three bedload samplers' efficiency in a gravel-bed river, Spitsbergen. *Geomorphology* **2017**, *287*, 90–100. [CrossRef]
52. Kendall, M.G. *Rank Correlation Methods*, 4th ed.; Charles Griffin: London, UK, 1975.
53. Mann, H.B. Nonparametric tests against trend. *Econometrica* **1945**, *13*, 245–259. [CrossRef]
54. Yue, S.; Wang, C. The Mann-Kendall test modified by effective sample size to detect trend in serially correlated hydrological series. *Water Resour. Manag.* **2004**, *18*, 201–218. [CrossRef]
55. Shi, H.; Hu, C.; Wang, Y.; Liu, C.; Li, H. Analyses of trends and causes for variations in runoff and sediment load of the Yellow River. *Int. J. Sediment Res.* **2017**, *32*, 171–179. [CrossRef]
56. Mama, R.; Jung, K.; Bidorn, B.; Namsai, M.; Feng, M. The local observed trends and variability in rainfall indices over the past century of the Yom River Basin, Thailand. *J. Korean Soc. Hazard Mitig.* **2018**, *18*, 41–55. [CrossRef]
57. Li, Z.; Xu, X.; Yu, B.; Xu, C.; Liu, M.; Wang, K. Quantifying the impacts of climate and human activities on water and sediment discharge in a karst region of Southwest China. *J. Hydrol.* **2016**, *542*, 836–849. [CrossRef]
58. Searcy, J.K.; Hardison, H.H. *Double-Mass Curves, Manual of Hydrology: Part 1, General Surface Water Techniques*; US Geological Survey: Washington, DC, USA, 1960; pp. 1–66.
59. Gao, P.; Li, P.; Zhao, B.; Xu, R.; Zhao, G.; Sun, W.; Mu, X. Use of double mass curves in hydrologic benefit evaluations. *Hydrol. Process.* **2017**, *31*, 4639–4646. [CrossRef]
60. Thiessen, A.H. Precipitation averages for large areas. *Mon. Weather Rev.* **1911**, *39*, 1082–1084. [CrossRef]
61. Moriasi, D.N.; Arnold, J.G.; Van Liew, M.W.; Bingner, R.L.; Harmel, R.D.; Veith, T.L. Model evaluation guidelines for systematic quantification of accuracy in watershed simulations. *Hydrol. Process.* **2007**, *50*, 885–900.
62. Bidorn, B.; Kish, S.A.; Donoghue, J.F.; Huang, W.; Bidorn, K. Variability of the total sediment supply of the Chao Phraya River, Thailand. River Sedimentation. In Proceedings of the 13th International Symposium on River Sedimentation, Stuttgart, Germany, 19–22 September 2016; CRC Press: Stuttgart, Germany, 2016.
63. Namsai, M.; Mama, R.; Sirapojanakul, S.; Chanyotha, S.; Phanomphongphaisan, N.; Bidorn, B. The characteristics of sediment transport in the upper and middle Yom River, Thailand. In Proceedings of the THA 2019 International Conference on Water Management and Climate Change towards Asia's Water-Energy-Food Nexus and SDGs, Bangkok, Thailand, 23–25 January 2019; Water Resources System Research Unit, Chulalongkorn University: Bangkok, Thailand, 2019; pp. 346–352.
64. Turowski, J.M.; Rickenmann, D.; Dadson, S.J. The partitioning of the total sediment load of a river into suspended load and bedload: A review of empirical data. *Sedimentology* **2010**, *57*, 1126–1146. [CrossRef]
65. Royal Irrigation Department (RID). *The Relation between Suspended Sediment and Drainage Area in 25 River Basins*; Royal Irrigation Department: Bangkok, Thailand, 2012. (In Thai)
66. Wu, C.; Ji, C.; Shi, B.; Wang, Y.; Gao, J.; Yang, Y.; Mu, J. The impact of climate change and human activities on streamflow and sediment load in the Pearl River basin. *Int. J. Sediment Res.* **2019**, *34*, 307–321. [CrossRef]
67. Panda, D.K.; Kumar, A.; Mohanty, S. Recent trends in sediment load of tropical (Peninsular) river basins of India. *Glob. Planet. Chang.* **2011**, *75*, 108–118. [CrossRef]
68. Li, D.; Lu, X.X.; Yang, X.; Chen, L.; Lin, L. Sediment load responses to climate variation and cascade reservoirs in the Yangtze River: A case study of the Jinsha River. *Geomorphology* **2018**, *322*, 41–52. [CrossRef]
69. Guo, L.P.; Mu, X.M.; Hu, J.M.; Gao, P.; Zhang, Y.F.; Liao, K.T.; Bai, H.; Chen, X.L.; Song, Y.J.; Jin, N. Assessing impacts of climate change and human activities on streamflow and sediment discharge in the Ganjiang River Basin (1964–2013). *Water* **2019**, *11*, 1679. [CrossRef]
70. Graf, W.L. Downstream hydrologic and geomorphic effects of large dams on America rivers. *Geomorphology* **2006**, *79*, 336–360. [CrossRef]
71. Royal Irrigation Department (RID). *Nan River Basin Development Feasibility Report Uttaradit Irrigation Project and Phitsanulok Irrigation Project*; Royal Irrigation Department: Bangkok, Thailand, 1970.
72. Land Development Department (LDD). *Status of Soil Erosion in Thailand*; Land Development Department: Bangkok, Thailand, 2020. (In Thai)
73. Kitisuntorn, P. Sediment Transport and Navigation Problem in Lower Nan River. Ph.D. Thesis, Department of Water Resources Engineering, Chulalongkorn University, Bangkok, Thailand, 1994. (In Thai).
74. Brune, G.M. Trap efficiency of reservoirs. *Eos Trans. Am. Geophys. Union* **1953**, *34*, 407–418.